Phase transitions in polyphosphazenes

S. G. Young, M. Kojima, J. H. Magill* and F. T. Lin†
School of Engineering and †Department of Chemistry, University of Pittsburgh, Pittsburgh, PA 15261, USA
(Received 12 July 1991; accepted 10 October 1991)

Halogenated phenoxyphosphazenes have been prepared by solution polymerization and characterized by g.p.c., d.s.c., Fourier transform i.r. spectroscopy, optical microscopy, solution and solid state n.m.r., dilatometry and diffraction techniques (WAXS and electron diffraction). Phase transitional behaviour was monitored above the thermotropic transition [$T(1)$] for each polymer and a general transformation scenario was established depending upon side group chemistry. It has been determined that side group size and substitution affects the glass transition temperature (T_g), $T(1)$ and the melting temperature (T_m) in a way that can be scaled linearly with $T(1)/T_m$ providing a useful guide to polyphosphazene behaviour. Through measuring properties as a function of temperature, a unifying perspective of the transitional characteristics of PB(4-H)PP and PB(3-H)PP polymers below as well as above $T(1)$ has been established. A smectic mesophase where the chain backbone is extended and packed (accommodated) into pseudohexagonal arrays is primarily responsible for the properties of polyphosphazene above $T(1)$. This arrangement also facilitates the ability of the thermotropic state to organize and solidify into an orthorhombic three-dimensional phase upon cooling from the two-dimensional thermotropic state. The polymers as crystallized from solution are of relatively low crystallinity in the monoclinic form, the level depends upon the nature and size of the side group and the conditions of precipitation.

(Keywords: polyphosphazenes; phase transitions; thermotropic)

INTRODUCTION

Phase transitions in thermotropic polyphosphazenes have created considerable interest in recent years and many experimental techniques[1–7] have been used to monitor them. Monitoring probes have included optical inspection of specimens between crossed polars using hot stage microscopy, d.s.c. (which is one of the more popular procedures) and ^{13}C and ^{31}P magic angle spinning (MAS) n.m.r. with decoupling as a recent and important method for *in situ* investigations. X-ray diffraction (WAXS and SAXS), TEM and SEM, as well as optical microscopy, have also featured strongly as important investigative procedures. Changes in significant physical behaviour as a function of temperature also include dynamic mechanical property[8] and creep measurements[9], and dielectric[10] and diffusion[11,12] studies. Much of the research emphasis has centred around the changes that occur in the polyphosphazenes prepared by solution casting and subsequent heat cycling through the thermotropic transition [$T(1)$] and beyond to the final isotropization or melting temperature (T_m). While many important and intriguing aspects of phase behaviour and concomitant morphological features have been studied, more details remain to be documented in order to improve our understanding of properties and morphology as they relate to modifying polymeric behaviour. Some of the interrelationships provide striking contrasts as well as similarities in polyphosphazenes. This paper reports on aspects of such a study for phenoxy-substituted polyphosphazenes of varying group size, polarity and chemistry by employing structure and morphological sensitive probes that monitor changes in physical characteristics with temperature.

One significant feature that precedes all physical measurements is proof of chemical structures (i.e. characterization), which is also emphasized in this paper.

EXPERIMENTAL

Materials

Several polyphosphazenes with phenyl and halogenated phenyl groups have been synthesized, purified and characterized. Solution polymerization[13] was employed. The characterization methods include g.p.c., solution ^{13}C and ^{31}P n.m.r., i.r. spectroscopy and elemental analysis. From these techniques, it was established that the polymers used were linear and free of side group or crosslinking impurities within the sensitivity limits of the analytical procedures.

G.p.c. measurements

G.p.c. measurements for our solution polymerized polyphosphazenes all exhibit polydispersities that are much lower than the corresponding melt polymerized polymers. This is clearly depicted in *Table 1*, which shows that the M_w/M_n ratios of the polyphosphazenes are usually $< \sim 4$.

Differential scanning calorimetry

D.s.c. measurements for physical investigations proved to be a good procedure for rapid detection of transitions

*To whom correspondence should be addressed. Present address: Office of Naval Research, 223-231 Old Marylebone Road, London NW1 5TH, UK

0032-3861/92/153215-11

Table 1 Results of the g.p.c. analysis for the poly[bis(halophenoxy) phosphazenes]

Polymer	M_n ($\times 10^{-5}$)	M_w ($\times 10^{-5}$)	M_w/M_n
Solution polymerization[a]			
PB(4-F)PP	6.6	25.8	3.9
PB(4-Cl)PP	4.4	17.9	4.1
PB(4-Br)PP	4.3	15.5	3.6
PB(3-F)PP	4.6	14.4	3.2
PB(3-Cl)PP	3.7	8.9	2.4
PB(3-Br)PP	6.6	23.3	3.5
Melt polymerization[a]			
PB(4-Cl)PP	3.2	35.6	11.3
PB(3-Cl)PP	2.2	21.3	9.7

[a]Given for comparison purposes

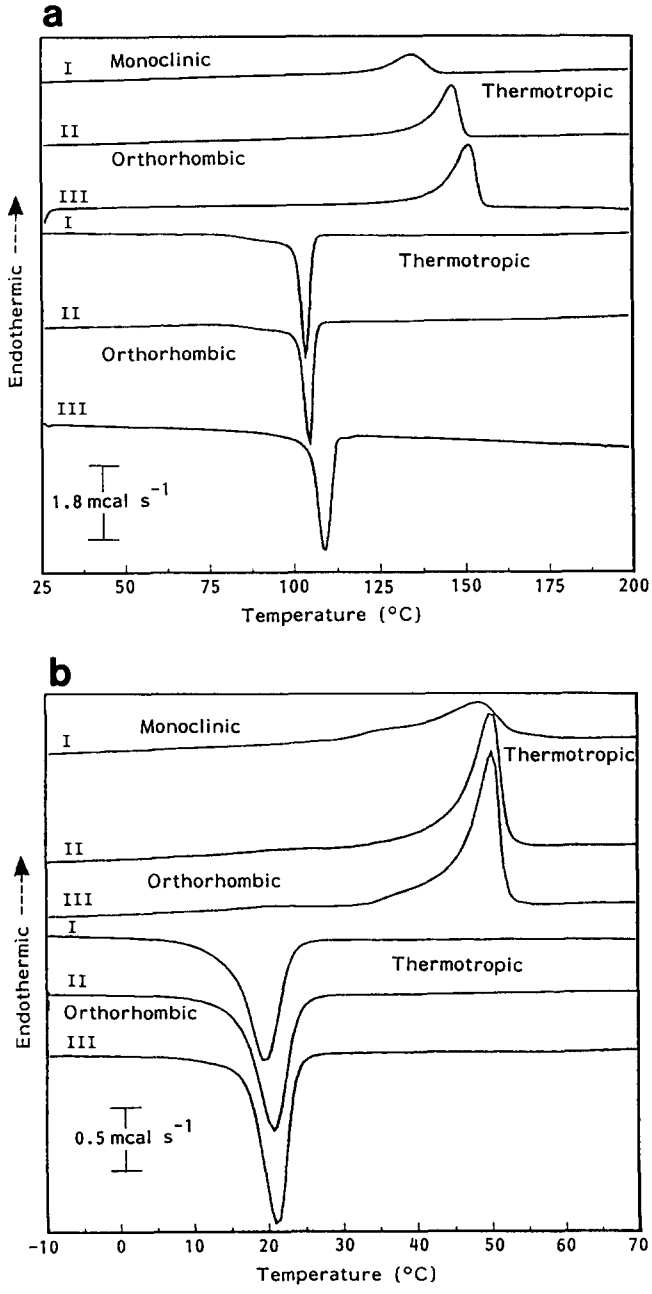

Figure 1 (a) D.s.c. heating/cooling curves (10°C min^{-1}) for poly[bis(*p*-fluorophenoxy)phosphazenes] between 25°C and 200°C: I, solution cast film; II, after heating/cooling I; III, after annealing at 200°C (30 min). (b) D.s.c. heating/cooling curves (10°C min^{-1}) for poly[bis(*m*-fluorophenoxy)phosphazenes] between 25°C and 200°C. Heat treatment conditions as in I–III in (a)

of diverse kinds, but especially for glass transition temperature (T_g), $T(1)$ and T_m detection. *Figure 1a* illustrates some results found for poly[bis(*p*-fluorophenoxy)phosphazene] (PB(4-F)PP). Note that there is an upward shift in the location of $T(1)$ and in T_m with heat cycling of the polymer specimen. There is also an enhancement in the enthalpy of these transitions except for the T_g region which decreases in intensity, but not location, with heating/cooling of the sample through $T(1)$ or T_m. A significant change in the breadth, area and position of the $T(1)$ transition occurs in a manner to be associated with structural and morphological transformations arising from diverse heat treatments. *Figure 1b* illustrates the transitional behaviour of poly[bis(*m*-fluorophenoxy)phosphazene] where similar trends are observed.

Interestingly, an important relationship exists between T_g, $T(1)$ and T_m for all the polymers studied here and elsewhere. *Figure 2* highlights this correlation for the polyphosphazenes. Some pertinent results obtained for *m*-substituted polyphosphazenes are listed in *Table 2*. Data for the PB(4-H)PP halo *p*-substituted phosphazenes are provided in *Table 3*.

Differential thermogravimetric analysis

Another well established monitoring technique, namely thermogravimetric analysis (t.g.a.), was used to determine the thermal stability of each polymer. This analysis was used in a routine manner in order to ascertain the stability of the polymer in nitrogen (this gas was employed as a 'blanket' in other measurements unless the polyphosphazene was being investigated under vacuum).

Dilatometry

This technique is well known, but it is also informative particularly in any investigation of transitional behaviour that is accompanied by a measurable change in volume. For this reason, it seems to be suitable for investigating all of the polyphosphazenes employed in this work. Dried specimens of solution precipitated polyphosphazenes

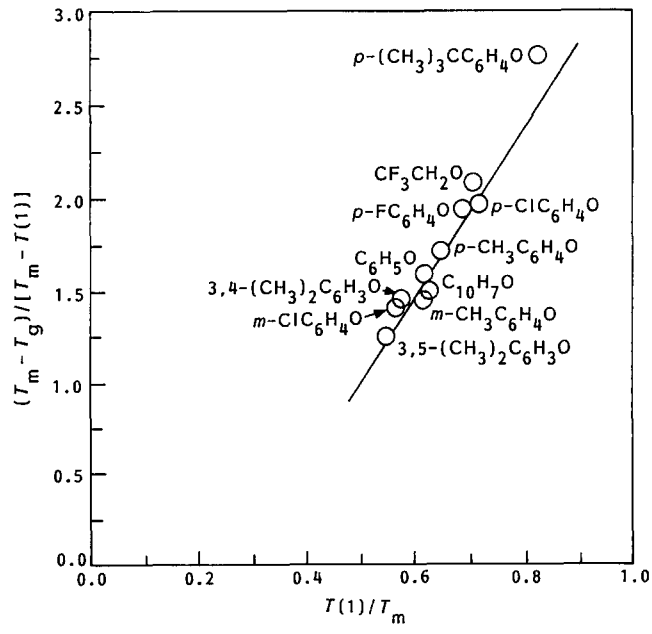

Figure 2 Plot of reduced parameters for polyphosphazenes (this work)

Table 2 Results of d.s.c. measurements for poly[bis(*m*-halophenoxy)phosphazenes]

		THF cast PB(3-H)PP films					
Polymer	Polymer history[a]	T_g (°C)	ΔC_p (cal g^{-1} K^{-1})	$T(1)$ (°C)	$\Delta H_{T(1)}$ (cal g^{-1})	T_c (°C)	T_m (°C)
PB(3-F)PP	I	−38	0.080	48	2.1	20	260
	II			49	4.0	21	
	III			50	4.0	21	
PB(3-Cl)PP	I	−24	0.074	66	2.5	35	290
	II			74	3.3	36	
	III			75	6.3	36	
PB(3-Br)PP	I	−15	0.044	81	3.7	35	320
	II			78	2.9	36	
	III			80	4.9	38	

[a]I, as-cast; II, second run after heating to 200°C and cooling to room temperature at 10°C min^{-1}; III, sample annealed at 200°C for 30 min and cooled to room temperature at 2°C min^{-1} before d.s.c. run

Table 3 Results of d.s.c. measurements for poly[bis(*p*-halophenoxy)phosphazenes]

		THF cast PB(4-H)PP films					
Polymer	Polymer history[a]	T_g (°C)	ΔC_p (cal g^{-1} K^{-1})	$T(1)$ (°C)	$\Delta H_{T(1)}$ (cal g^{-1})	T_c (°C)	T_m (°C)
PB(4-F)PP	I	−2	0.063	134	3.1	103	370
	II			146	6.9	105	
	III			151	9.0	109	
PB(4-Cl)PP	I	4	0.023	150	3.7	139	390
	II			171	7.1	141	
	III			173	7.4	143	
PB(4-Br)PP	I	24	0.076	156	2.0	131	420
	II			164	4.7	132	
	III			166	5.0	134	

[a]See footnote to *Table 2*

were fabricated as transparent cylindrical discs under both pressure and vacuum to yield transparent void-free plugs that were introduced into the dilatometer head and sealed before the dilatometer assembly was filled with triply distilled mercury that was introduced under vacuum following the standard evacuation procedure. After adjustment of the mercury to a level judged appropriate for the experiment, the assembly was immersed in a thermostatically controlled silicone oil bath and ramp heated slowly through the $T(1)$ transition in a manner that was appropriate for the polymer in question. After approximately every 5°C, the bath was thermostatically controlled to within ±0.05°C of the set temperature and the mercury height was recorded (on a rising meniscus) at equilibrium. Cooling measurements were also carried out stepwise in a similar fashion. Typical heating/cooling curves are illustrated in *Figure 3*. In *Figure 3*, poly[bis-(trifluoroethoxy)phosphazene] (PBFP) and poly[bis-(phenoxy)phosphazene] (PBPP) polymers are employed as reference materials. Each polymer was subjected to several thermal cycles. The specific volume in the initial run was always found to be considerably higher than the values encountered in subsequent measurements. The magnitude of the transition in volume obtained in this first run is always lower than is found in subsequent runs after heat cycling. The temperature span of the first transition is always broad for morphological and kinetic reasons that will be addressed later.

The expansion coefficients determined for halogenated phenoxy compounds are given in *Table 4*. The first column α_c is determined for the crystalline orthorhombic phase established after the first heating, the $\alpha_{T(1)}$ values were calculated from the specific volume–temperature lines for the thermotropic phase above $T(1)$:

$$\alpha_i = \frac{1}{v_i}\left(\frac{\delta v_i}{\delta T}\right)P$$

where i denotes the appropriate phase.

Density gradient column measurements

The liquids used in constructing this column were ethanol (density, $\rho = 0.79$ g ml^{-1}) and carbon tetrachloride ($\rho = 1.60$ g ml^{-1}). The column was calibrated with glass floats of known ρ (± 0.001 g ml^{-1}) to provide a linear relationship (correlation coefficient ~0.9999) between ρ (g ml^{-1}) and height (cm) in the column. The column was controlled to better than ±0.05°C. The ρ values of small dried samples of polyphosphazene (<1 mm^3) were measured in this column and cross-checks were made with dilatometry data and with variously heat-treated specimens used for X-ray and other measurements.

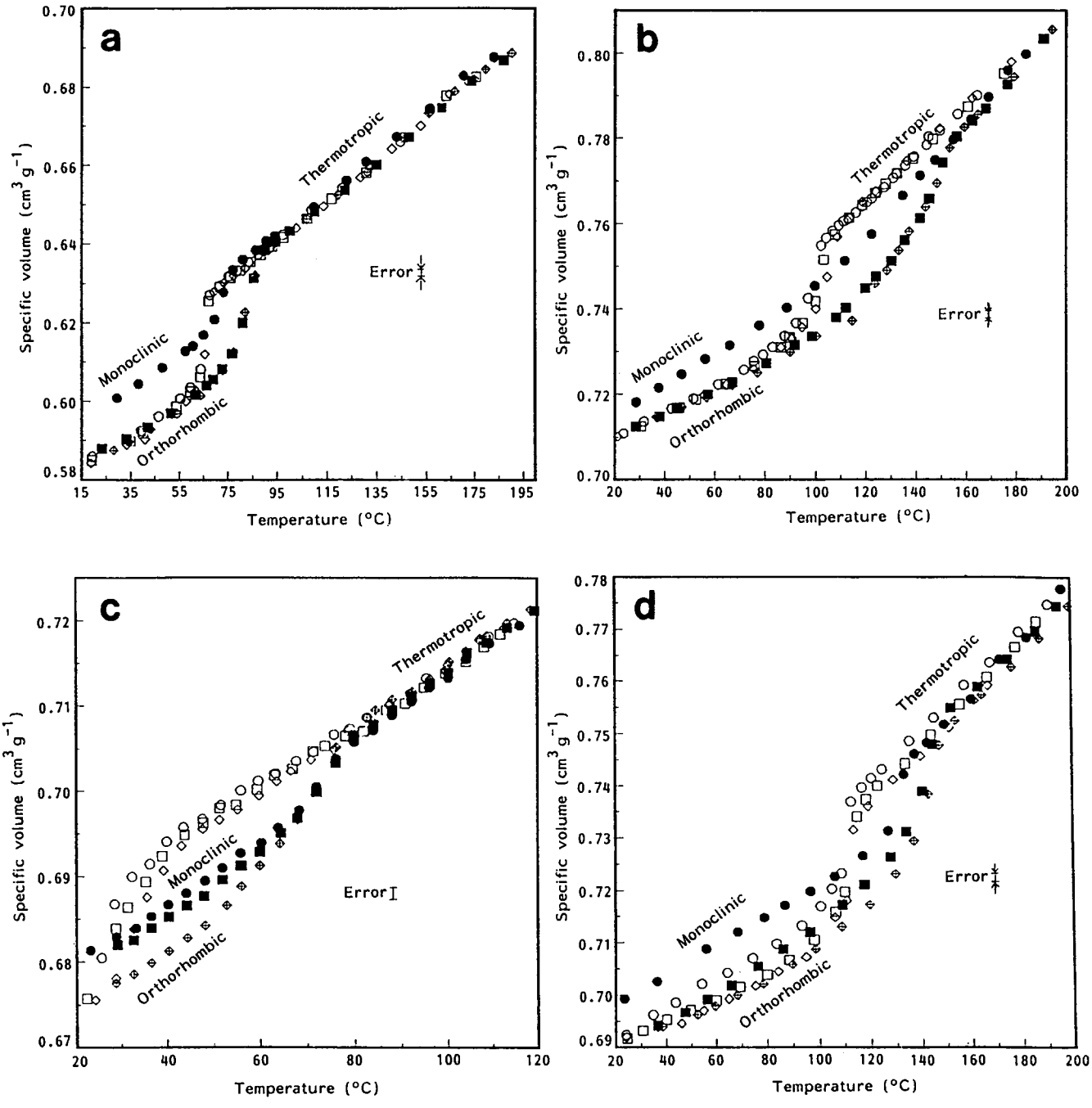

Figure 3 Specific volume *versus* temperature plots for (a) PBFP, (b) PBPP, (c) PB(3-Cl)PP and (d) PB(4-F)PP. Temperature ranges vary with the polymer and its $T(1)$ transition: (●) first heating; (○) first cooling; (■) second heating; (□) second cooling; (⊕) third heating; (◇) third cooling

Spectroscopy

Transmission Fourier transform i.r. (*FT*i.r.) spectra were obtained from 1600 to 400 cm^{-1} for each polymer. A Mattson Polaris *FT*i.r. instrument with a liquid nitrogen cooled detector was employed with an IBM computer for data acquisition. All spectra exhibited similar features with no noticeable P–O–P stretching or bending so testifying to the linearity of the polymers in accordance with other means of characterization. Likewise, no P–OH bonds were detected, which is evidenced by lack of the 2550–2700 and 2100–2300 cm^{-1} characteristic bands. Typical spectra are illustrated in *Figures 4a* and *b* for PB(3-H)PP and PB(4-H)PP type polyphosphazenes, respectively. The vibrational bond assignments have approximately the same locations as in the spectrum of PBPP (*Figure 4c*). The principal band assignments are indicated in the figures.

Solution n.m.r. spectroscopy

Investigations were carried out using a Brüker AM 500 n.m.r. spectrometer with an operating frequency of 202 MHz for ^{31}P and 125 MHz for ^{13}C measurements. Solution ^{31}P n.m.r. spectroscopy was used to determine that a linear polymer was synthesized and ^{13}C n.m.r. spectroscopy was employed to demonstrate that the desired side groups were attached to the backbone of the particular polyphosphazene.

All solution ^{13}C n.m.r. spectra were recorded in two different modes namely, ^{1}H coupled and decoupled. Tetramethylsilane (0 ppm reference) was employed as a

Table 4 Expansion coefficient data for some polyphosphazenes

Polymer	α_c ($\times 10^4$) (K^{-1})	$\alpha_{T(1)}$ ($\times 10^4$) (K^{-1})
PB(3-F)PP	6.7	6.6
PB(3-Cl)PP	7.0	6.9
PB(3-Br)PP	7.4	7.3
PB(4-F)PP	5.4	11.2
PB(4-Cl)PP	6.4	12.7
PB(4-Br)PP	9.7	21.3
PBPP	6.0	10.6
PBFP	8.9	10.7

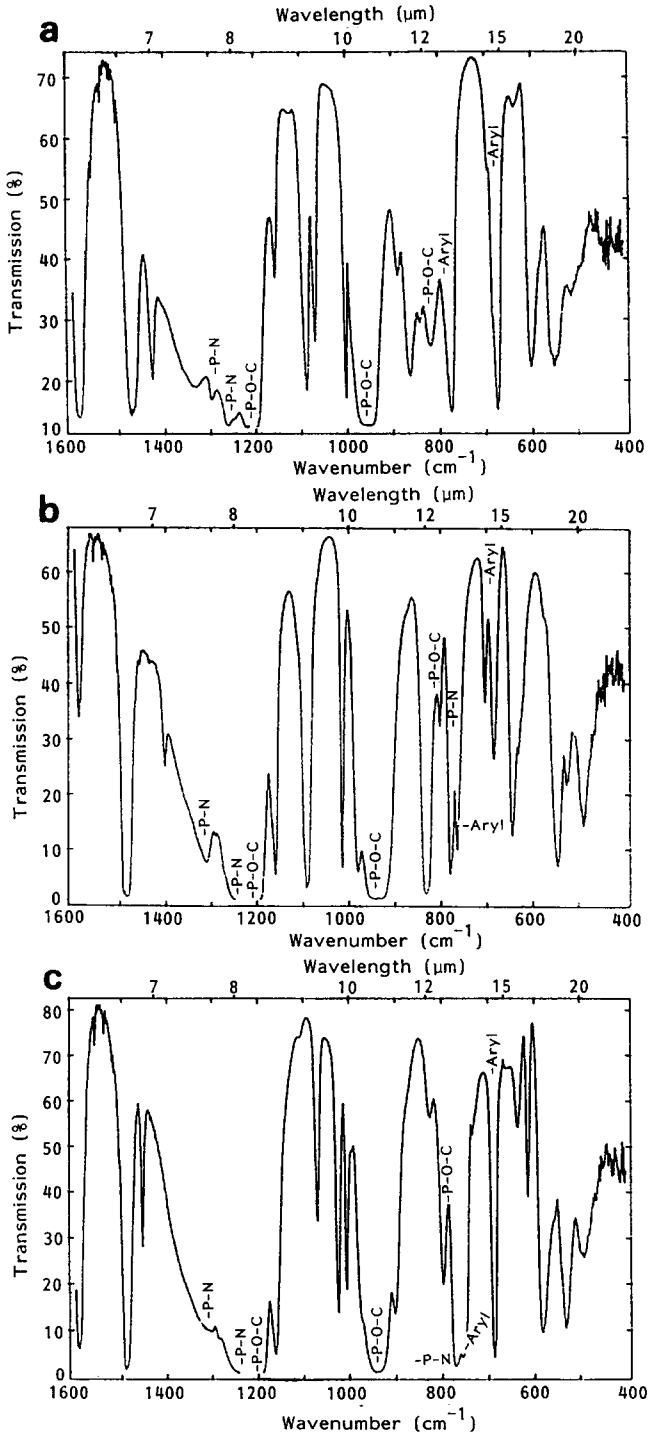

Figure 4 I.r. spectrum of a typical PB(4-H)PP and PB(3-H)PP polymer in the transmittance mode showing the principal peaks: (a) poly[bis(*m*-chlorophenoxy)phosphazene]; (b) poly[bis(*p*-chlorophenoxy)phosphazene]; (c) poly[bis(phenoxy)phosphazene]

reference standard (0 ppm). *Figure 5* gives typical spectra for PB(4-Br)PP and PB(3-Br)PP in the coupled and decoupled modes. A summary of ^{13}C n.m.r. resonances for poly(phenoxy)phosphazenes and their corresponding assignments are shown in *Table 5* for each carbon atom in the phenyl side chain. Results of ^{31}P n.m.r. analysis for polyphosphazenes are listed in *Table 6*. From these results, it can be concluded that the chemical structures as stated, complement the *FT*i.r. and other means of polyphosphazene characterization.

Solid state n.m.r. spectroscopy

Solid state variable temperature MAS n.m.r. measurements were made using a Brüker MSL 300 spectrometer with an operating frequency of 121.5 MHz for ^{31}P and 75.5 MHz for ^{13}C analysis. Magic angle sample spinning was performed at speeds of 2.0–4.0 kHz. The instrument temperature capability ranged from 100°C down to cryogenic values. Dried solution crystallized powder of each polyphosphazene was spun in aluminium oxide rotors inside the sample chamber during stepwise heating/cooling and then isothermal holding of the polymer during measurement times that were spaced at 5–10°C intervals approximately.

A series of MAS n.m.r. measurements and results show that this technique is useful for the study of *in situ* molecular chain dynamics, chain conformation and specimen crystallinity of polyphosphazenes. Often, an ordered (crystalline) and a disordered (amorphous) contribution are exhibited by the chain backbone below $T(1)$, whereas above this temperature a single highly mobile two-dimensional (2-D) phase exists in an expanded state depicted by dilatometry measurements. Clearly, there is a strong crystallinity dependence upon temperature (*Figure 6*), as has been noted[14] and also

Table 5 Summary of the ^{13}C n.m.r. analysis for poly[bis(halophenoxy) phosphazenes]

Polymer	^{13}C n.m.r. (ppm)					
	C_1	C_2	C_3	C_4	C_5	C_6
PBPP	152.7	122.1	129.7	124.4	129.7	122.1
PB(4-F)PP	148.0	116.5	123.1	161.3 159.3	123.1	116.5
PB(4-Cl)PP	130.8	122.9	130.2	150.4	130.2	122.9
PB(4-Br)PP	118.5	123.2	133.3	151.0	133.3	123.2
PB(3-F)PP	152.7	131.0	164.6 162.6	117.4	109.4	112.4
PB(3-Cl)PP	135.2	131.0	152.3	125.9	119.8	121.9
PB(3-Br)PP	123.0	131.3	152.2	128.7	120.2	124.7

Table 6 Results of the ^{31}P n.m.r. analysis for the polyphosphazenes synthesized

$[-P(R)_2=N-]_n$	
Side group R	^{31}P (ppm)
OCH_2CF_3	−6.9
OC_6H_5	−20.1
OC_6H_4-(*p*)-F	−16.2
OC_6H_4-(*p*)-Cl	−17.0
OC_6H_4-(*p*)-Br	−17.0
OC_6H_4-(*m*)-F	−17.8
OC_6H_4-(*m*)-Cl	−17.5
OC_6H_4-(*m*)-Br	−17.5

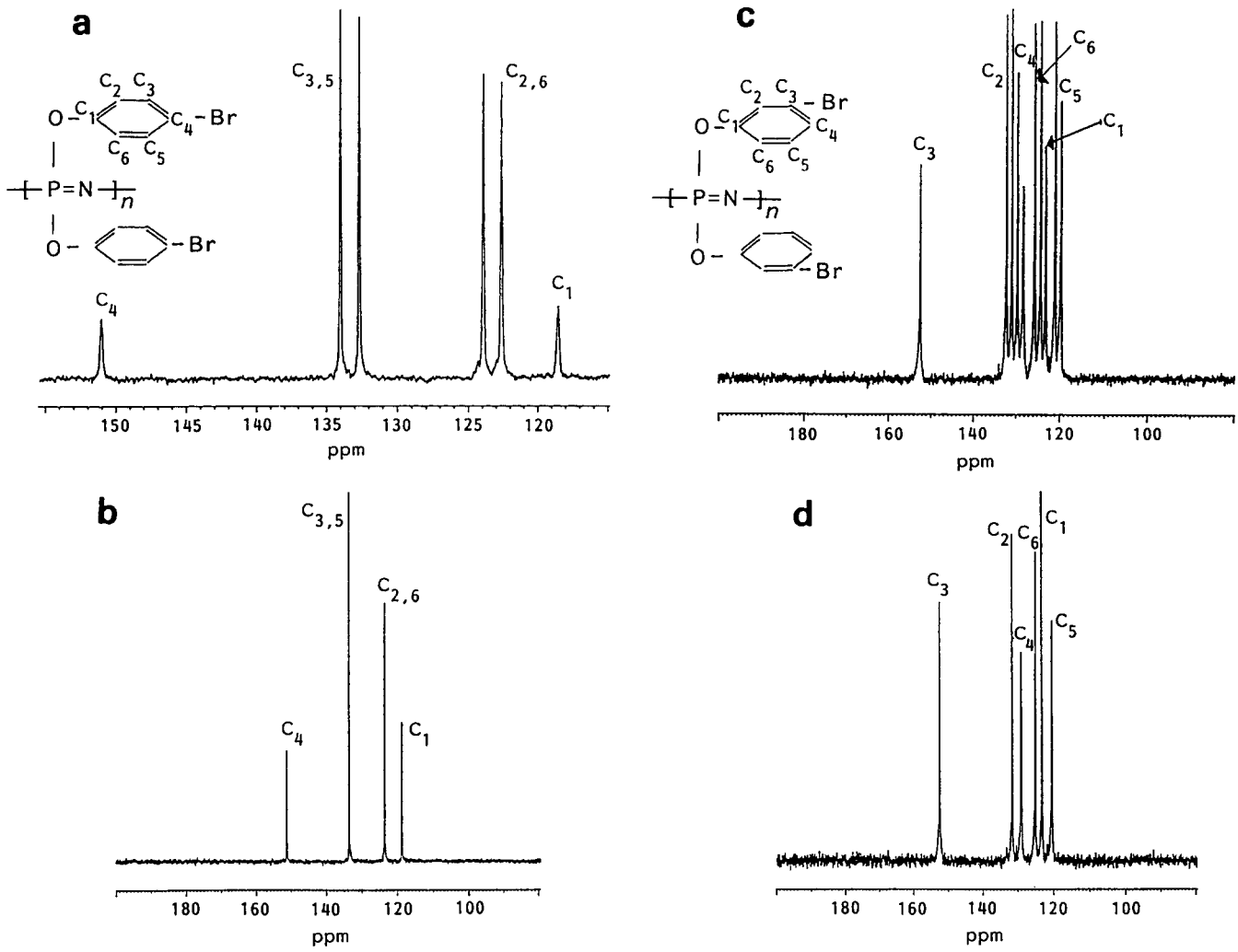

Figure 5 ^{13}C n.m.r. spectra of PB(4-Br)PP: (a) ^{1}H coupled; (b) ^{1}H decoupled. ^{13}C N.m.r. spectra of PB(3-Br)PP: (c) ^{1}H coupled; (d) ^{1}H decoupled

recorded in d.s.c. and X-ray measurements[15]. Still, all of the results are not as well defined as in PBFP where the side groups are relatively small and inherently mobile (by n.m.r.) because the T_g of the polymer is well below room temperature. Even so, there seems to be a common pattern (with some exceptions *Figures 7a* and *b*). This will be addressed in the discussion.

Elemental analysis

These analyses are provided in *Table 7* and attest to the chemistry of the polyphosphazenes synthesized.

DISCUSSION

T(1) transition

Trends in physical parameters of several well characterized poly[bis(halophenoxy)phosphazenes] have been measured and categorized: several unifying trends or features are evident in this work.

Specifically, the observed d.s.c. changes (*Figures 1a* and *b*) that occur upon temperature cycling through $T(1)$ in these polyphosphazenes are as follows:

1. upon the initial ramp heating a relatively small and broad transition is noted for the solution cast monoclinic phase which is chain folded crystalline ($<50\%$) with amorphous or disordered regions. This peak area is a compromise associated with the enthalpy of 'melting' and concomitant chain extension into the expanded thermotropic phase (as labelled);
2. upon cooling from the thermotropic state the crystallization peak narrows (as expected) and this change is associated with the enthalpy difference between the 2-D thermotropic and the three-dimensional (3-D) orthorhombic forms that possess some inherent disorder (verified by X-ray, electron diffraction and other techniques) depending upon cooling conditions;
3. in subsequent heating the $T(1)$ transition is enlarged and sharpened and occurs at a higher temperature;
4. on cooling again, the crystallization curve appears earlier on the temperature scale and its peak area is also enhanced;
5. on further recycling the enhancements in these parameters become less pronounced, since 3-D ordering occurs below, and 2-D disordering takes place at $T(1)$, and each state improves asymptotically, i.e. shifts with heat treatment as demonstrated already for other polyphosphazenes[8,14,16].

Figure 2 establishes that the side group dimensions may be correlated linearly with the characteristic parameters T_g, $T(1)$ and T_m determined by d.s.c. or other

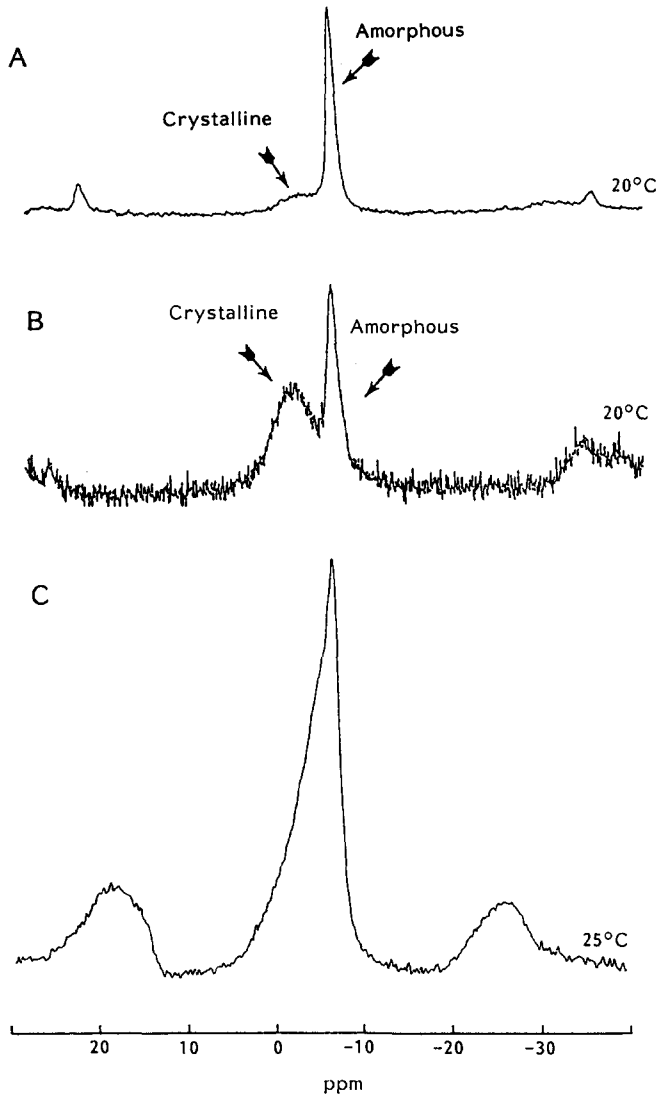

Figure 6 Solid state MAS ^{31}P n.m.r. spectra of PBFP: (A) initially as precipitated from solution, 20°C; (B) after heating to 100°C in the Brüker spectrometer and cooling to 20°C; (C) after annealing outside the spectrometer in nitrogen at 200°C and measured at 25°C

means. These fundamental parameters are intrinsically associated with side chain chemistry and polyphosphazene characteristics. The location and magnitude of the $T(1)$ peak changes significantly with temperature cycling. The broad peak depicted initially in *Figure 1* (e.g. run I) relates to a sample of relatively low initial crystallinity ($<50\%$) having a chain folded lamellar spherulitic morphology that was formed by solution crystallization. These general features were found to be characteristic of all the polyphosphazenes, the specimen crystallinity decreases with increasing side group dimensions and their reduced role in influencing crystallizability. The folded morphology of the monoclinic form necessarily unfolds in the vicinity of $T(1)$ during the first d.s.c. run. The transformation is driven by entropic disordering of side groups so as to relieve induced stress and so produce a more stable and open chain extended thermotropic morphology that is controlled by side group conformations (or the lack thereof) through the $T(1)$ temperature. After $T(1)$ is reached the polymer chains become extended and occupy a pseudohexagonal arrangement presumably in diverse sized domains that are not yet identified *per se* in this investigation. There is considerable side group and even backbone mobility above $T(1)$ according to solid state MAS n.m.r. measurements made during temperature cycling through the $T(1)$ transition. Complementary less direct evidence

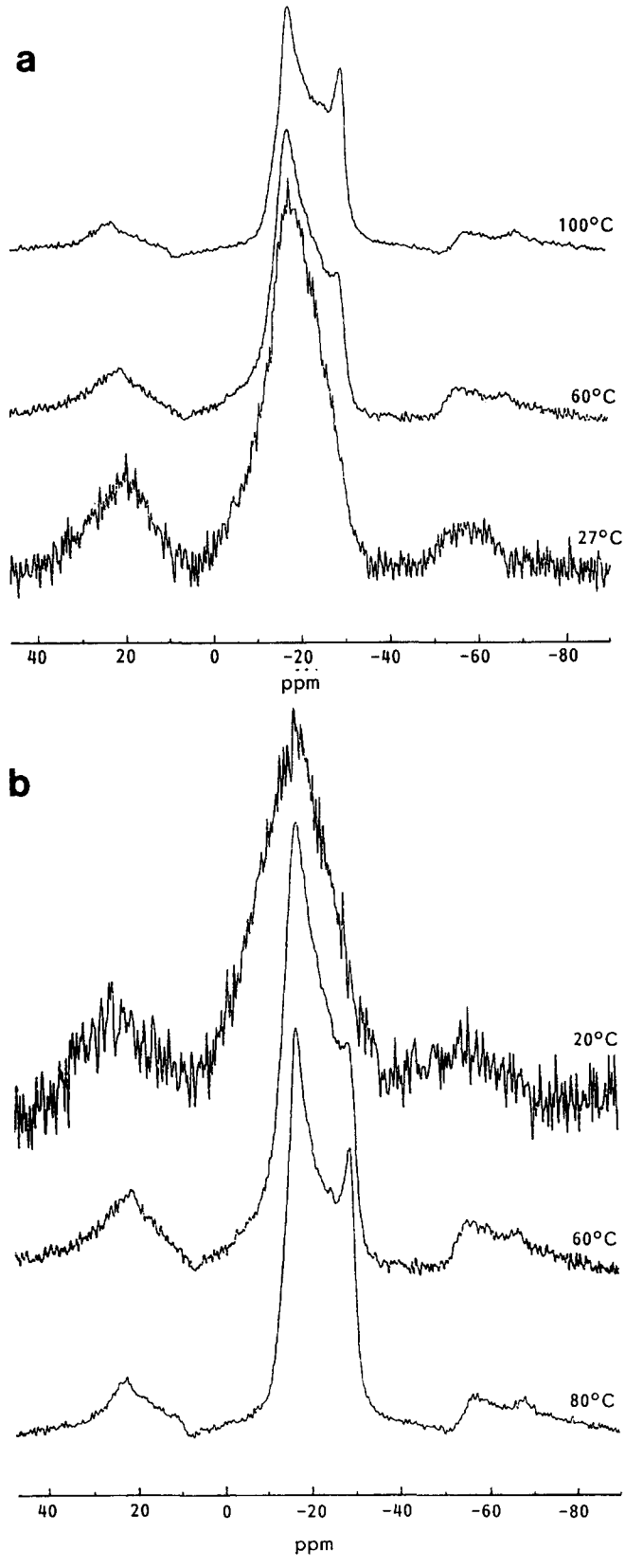

Figure 7 ^{31}P n.m.r. spectra of PB(3-Br)PP obtained during (a) heating and (b) cooling between room temperature and 100°C, respectively

Table 7 Some elemental analyses of PBHPP type polyphosphazenes

Substituent	C	N	P	F	Cl	Br	H	O	%
4Cl	48.5	4.4	10.3	–	22.7	–	–	–	Found
	48.0	4.7	10.3	0	23.6	0	2.7	10.7	Calc.
4Br	37.0	3.5	7.7	–	<0.4	40.7	–	–	Found
	37.1	3.6	8.0	0	0	41.1	2.1	8.2	Calc.
3Cl	48.2	5.1	–	–	–	–	2.6	–	Found
	48.0	4.7	10.3	0	23.6	0	2.7	10.7	Calc.
3Br	38.9	3.9	–	–	–	–	2.3	–	Found
	37.1	3.6	8.0	0	0	41.1	2.1	8.2	Calc.
4F	54.2	–	10.5	–	–	–	2.8	12.5	Found
	54.0	5.2	11.6	14.2	0	0	3.0	12.0	Calc.

All of the above showed no branching for ^{31}P solution n.m.r.; the i.r. spectra were normal too

is found in dilatometry and X-ray expansion measurements.

Transmission electron diffraction evidence made on metal shadowed thin monoclinic 'single crystal-like' morphologies below and above $T(1)$ provides direct evidence[17] for crystal thickening and surface roughening whenever crystals are heated through this transition. Likewise, small-angle X-ray diffraction measurements[18] made: (1) on original samples heated *in situ* and examined simultaneously using synchrotron SAXS radiation; and (2) by standard SAXS monitoring of samples[17] after stepwise heating/annealing, demonstrate that thickening occurs in the chain backbone direction whenever specimens are heated initially via the $T(1)$ transition. No further changes in SAXS long spacings were observed on subsequent thermal cycling or measurements. These results suggest that after the initial chain thickening as $T(1)$ is approached, the process is irreversible presumably because the chain extended morphology has greater stability than the folded monoclinic morphology. However, there is a need to make additional measurements whenever narrow molecular weight fractions become available, in order to establish this situation with a higher degree of certainty.

The extent of ordering improves greatly with temperature cycling as witnessed by the upward temperature shift in $T(1)$ and the enthalpy enhancement with annealing. Clearly, there is indisputable experimental evidence for this change and other observations reported in this paper support this trend in behaviour. The interchain spacing in the thermotropic state is controlled by the side group dimension on the phosphorus. The spacing increases in accordance with the increase in the size of the substituted phenoxy group or side group dimensions. The dimensional changes from X-ray diffraction[19] listed in *Table 8* evoke a pattern and follow it. The magnitude of the interchain spacing varies with heat treatment since not only does it depict side group packing in a 2_1 helical chain arrangement, but the rate of heating/cooling influences the actual conformation of the mesogenic side chains according to diffraction evidence[20–22], which is not always well-defined when the side groups are small. However, the clearest evidence comes from the dependence of side group dimensions that affects interchain spacing in the 2-D and 3-D states. These transformations are manifested in a less delicate fashion by significant volume changes that are observed via dilatometry, which monitors the average molecular

Table 8 Results of X-ray diffraction measurements for PB(4-H)PP at 200°C

Polymer	No.	I^a	d (Å)	(hkl)	a_s (Å)[b]
PB(4-F)PP	1	vs	11.5	(100)	13.2
	2	w	6.67	(110)	
	3	w, broad	~5.0	(210)	
PB(4-Cl)PP	1	s	12.3	(100)	14.2
	2	vw	7.16	(110)	
	3	w, broad	5.4	(210)	
PB(4-Br)PP	1	m	12.6	(100)	14.5
	2	vw	7.22	(110)	
	3	w, broad	5.4	(210)	

[a]Intensity: vs, very strong; s, strong; m, medium; w, weak; vw, very weak

[b]Intermolecular distance between chains in the thermotropic phase (at 200°C)

conformation in the bulk specimen and encompasses disordered as well as ordered states of the polymer that are dictated by sample history. The relative contributions from each of these factors cannot be deconvoluted to provide a clear picture of the overall transformation scenario measured by dilatometry unless sufficient knowledge of the amorphous/crystalline morphology (or state of order) of the system is available so that their relative contributions with temperature are known. Some characterization has been accomplished by X-ray and microscopical investigations of polyphosphazene specimens that have been removed from the dilatometer after specimens were subjected to known thermal histories.

Solid state n.m.r. spectroscopy

MAS n.m.r. analysis is often a useful probe used to study *in situ* conformational changes that occur within the polymer specimen during temperature cycling. It is a non-destructive test (that usefully complements diffraction and other techniques) used to monitor transformations that arise in the solid state under isothermal or temperature cycling. However, there are sometimes inherent complexities that arise in making comparisons between methods. Results obtained for PBFP, a trifluoroethoxyphosphazene, although reported[23] already in part, are still worth emphasizing since some of the fundamental changes that occur in morphology are better documented experimentally in

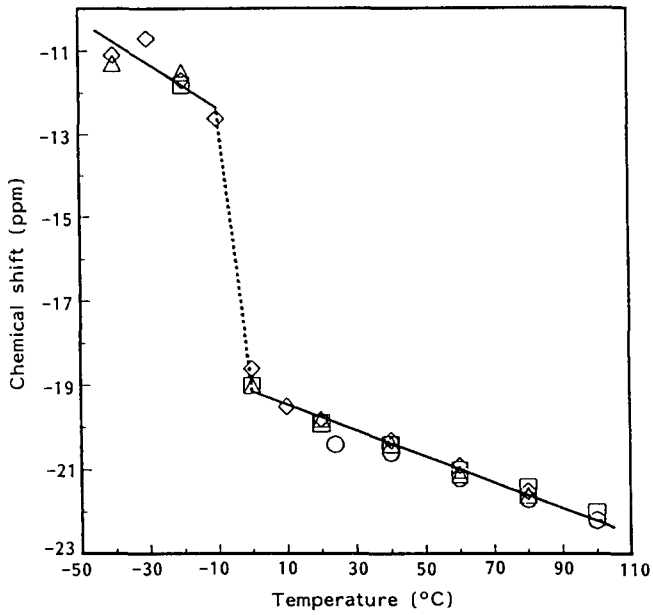

Figure 8 ^{31}P chemical shifts of PB(3-F)PP during thermal cycling: (○) first heating; (△) first cooling; (□) second heating; (◇) second cooling

PBFP (*Figure 6*) and are also of fundamental importance to the other polymers, where the side group is larger and less mobile, as in the halogenated phenoxyphosphazenes that usually have considerably higher T_g values (see *Tables 2* and *3*) compared to PBFP ($T_g \sim -66°C$). ^{31}P MAS n.m.r. results for all the halophenoxyphosphazenes support the idea of two resonances below $T(1)$, one belonging to the amorphous (disordered) regions and the other to the crystalline (ordered) regions of the polymers. *Figure 8* depicts the changes in the ^{31}P chemical shifts observed in PB(3-F)PP with temperature cycling. However, there are also different features noted for instance in the ^{31}P n.m.r. spectra of PB(3-Br)PP in *Figure 7a* at these selected temperatures on heating and in *Figure 7b* upon cooling to room temperature. Initially, a single broad peak is noted at 27°C. As the polymer is heated, a peak appears at −29 ppm, which corresponds to the $T(1)$ mesophase and two distinct peaks also coexist above this transition. Upon cooling the sample in the spectrometer, the −29 ppm resonance decreases and then disappears reversibly at 20°C. This behaviour contracts with the results of other polyphosphazenes and may be attributed to steric interactions involving the polar *m*-substituted bromine atom on the phenyl ring. Again, the time-scale of the experiment may not be adequate for the PB(3-Br)PP to reorganize properly into a 2-D mesophase as witnessed by the coexistence of two resonances above $T(1)$. X-ray diffraction evidence made on heat treated PB(3-Br)PP indicates that the low crystallinity solution precipitated monoclinic form transforms into the orthorhombic form, which then shows improved order upon stretching below $T(1)$. Other polyphosphazenes in this series exhibit similar behaviour in agreement with d.s.c., dilatometry and other measurements.

The ^{13}C cross-polarization (CP)/MAS spectra of the same polymer (*Figure 9*) taken at 25°C and 100°C, respectively, also exhibit behaviour that is distinct from the other polyphosphazenes. At 25°C two broad resonances are present [as in PB(3-Br)PP], but at 100°C one of these disappears and the other one splits into a doublet. This feature is probably an artifact of CP since this technique is designed for rigid systems[24]; PB(3-Br)PP is not a rigid system owing to its very low crystallinity. It seems that the bromine-substituted carbon is extremely mobile below and above $T(1)$, so that the ^{13}C resonances cannot be observed due to a time-averaged superposition. Further study will be devoted to resolve this complexity.

In the case of PB(3-F)PP, the ^{31}P chemical shift with temperature cycling is very reproducible and does not alter much between the first and second runs. A sharp step that occurs at $\sim -10°C$ seems to be related to a backbone conformational change. The downfield shift of this change signifies that the electron density of the backbone decreases substantially. Surprisingly, there is no step change at the $T(1)$ transition (49°C) or at T_g ($\sim -38°C$).

Again, the ^{13}C CP/MAS n.m.r. spectra for this PB(3-F)PP (like PBFP) exhibit side group mobility in the 3-D and 2-D phases. In the latter (thermotropic) state, the carbon atoms are slightly more mobile above 50°C. *Table 9* lists the ^{13}C spin-lattice relaxation times

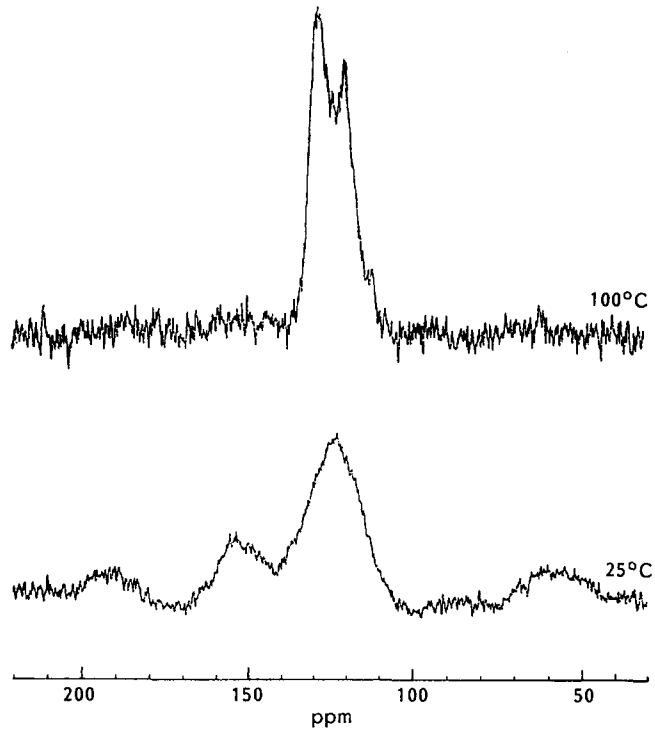

Figure 9 ^{13}C CP/MAS n.m.r. spectra of PB(3-Br)PP at 25°C and 100°C, respectively

Table 9 Results of the ^{13}C T_1 spin-lattice relaxation measurements (in s) for PB(3-F)PP

	Temperature (°C)	
Carbon atom	25	75
C_1	1.9	1.1
C_2	1.1	0.5
C_3	1.5	0.9
C_4	0.5	0.3
C_5	0.6	0.2
C_6	0.5	0.3

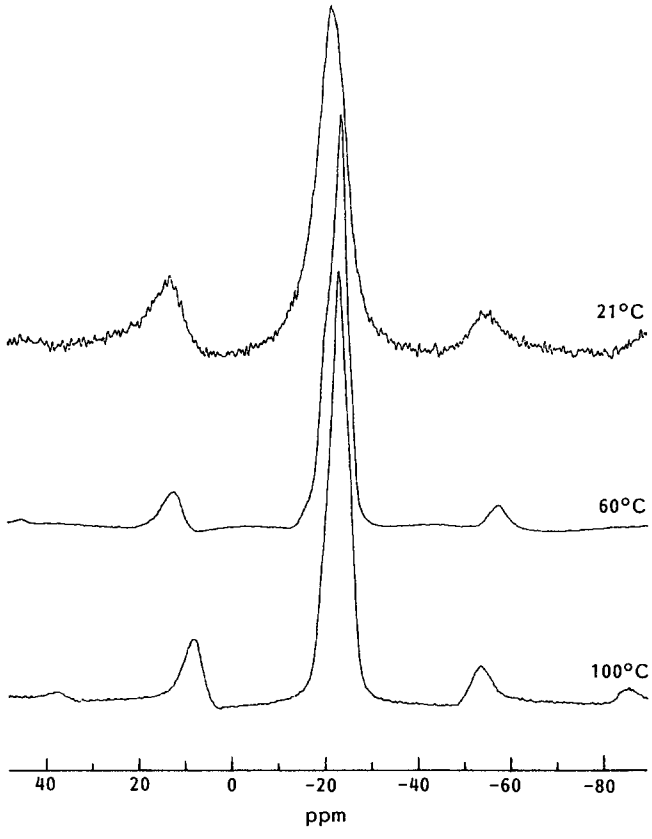

Figure 10 ^{31}P n.m.r. spectra of PB(3-Cl)PP during thermal cycling between room temperature and 100°C, respectively

for PB(3-F)PP at 25°C and 75°C, respectively. For the PB(3-Cl)PP polymer (*Figure 10*), with its $T(1)$ transition at 75°C and $T_g \sim -24$°C, ^{31}P n.m.r. spectra were recorded on heating/cooling. Only one ^{31}P n.m.r. resonance is observed on either side of $T(1)$ due to the fact that the electron density and magnetization of the phosphorus atoms in the backbone are similar in the 2-D and 3-D phases. From the ^{31}P chemical shift *versus* temperature no step change is observed at $T(1)$. The ^{13}C CP/MAS n.m.r. spectra only show two resonances even after 31 000 scans. One resonance can be assigned to the chlorine-substituted carbon with all the other resonances lumped into the other peak. Since none of the individual carbon resonances could be assigned, no relaxation measurements were possible. This behaviour may be attributed to an averaging of the magnetization of each carbon atom so that individual resonances overlap.

Measurements may be possible using oriented polyphosphazenes where it has been established recently[25] that very well-defined X-ray diffraction patterns may be obtained under the proper heat treatment and stretching conditions. Apparently, stress induces or enhances ordering, or crystallization, from the 2-D to the 3-D state more readily when specimens are stretched than it does in the relaxed state where steric and polar restrictions curtail the transformation *per se*, which is also very dependent upon kinetic considerations.

CONCLUSIONS

1. Halogenated phenoxyphosphazenes were prepared by solution polymerization procedures and well characterized as linear polymers using diverse techniques.
2. All solution crystallized polyphosphazenes precipitate in the monoclinic form in a state of low crystallinity (<50%). The larger the side group the lower is the degree of crystallinity in the precipitated crystals.
3. A unifying transformation scenario is evidenced for these polymers as follows with temperature cycling:

monoclinic (low 3-D crystallinity) (chain folded)	heating $>T(1)$ (chain unfolding and extension)	thermotropic 2-D (pseudohexagonal) smectic phase

   Cooling from above $T(1)$ to room temperature results in a chain extended 3-D orthorhombic phase of enhanced crystallinity wherein the side groups become accommodated in an orthorhombic unit cell, more especially and readily when samples are stretched.
4. Heat treatment [temperature cycling or annealing near or above $T(1)$] enhances chain and side group mobility that induces improved 2-D or 3-D order depending upon the rate of cooling of the polymer specimens.
5. The interchain spacing is strongly influenced by side group chemistry and dimensions so that the smectic layer spacing is controlled by side group size and 2_1 helical conformation.
6. MAS n.m.r., d.s.c. and X-ray results provide a self-consistent picture of transitional change with heating/cooling through $T(1)$.
7. T_g, $T(1)$ and T_m parameters scale in a manner that is consistent with the side group size and chemistry.
8. Order, above and below $T(1)$ depends upon sample history (time and temperature).

ACKNOWLEDGEMENTS

Partial support for this work was provided by the National Science Foundation (Materials Program) and the Office of Naval Research (Chemistry Program). Helpful discussions with Dr George Marcelin, School of Engineering, are gratefully acknowledged.

REFERENCES

1 Allcock, H. R. *Chem. Eng. News* 1985, 22
2 Sokolskaya, I. B., Friedzon, Y. S., Kochervinskii, V. V. and Shilbayev, V. P. *Polym. Sci. USSR* 1986, **38**, 239
3 Aharoni, S. M. *J. Macromol. Sci. Phys.* 1982, **B21**, 105
4 Magill, J. H., Petermann, J. and Rieck U. *Colloid Polym. Sci.* 1986, **264**, 570
5 Kojima, M. and Magill, J. H. *Makromol. Chem.* 1985, **186**, 649
6 Schneider, N. S., Desper, C. R., Singler, R. E., Alexander, M. and Sagalyn, P. L. in 'Organometallic Polymers' (Eds C. Carraher Jr, J. E. Sheats and C. U. Pittman Jr), Academic Press, New York, 1986, pp. 5, 271 *et seq.*
7 Gomez, M. A., Marco, C., Faton, J. G., Chichester-Hicks, S. V. and Haddon, R. C. *Polym. Commun.* 1980, **31**, 308
8 Choy, I. C. and Magill, J. H. *J. Polym. Sci., Polym. Chem. Edn* 1981, **19**, 2495
9 Masuko, T., Simeone, R. J., Magill, J. H. and Plazek, D. J. *Macromolecules* 1984, **17**, 2857
10 Uzaki, S., Adachi, K. and Kotaka, T. *Polym. J.* 1988, **20**, 221
11 Kajiwara, M. *J. Mater. Sci. Lett.* 1988, **7**, 102
12 Ciora Jr, R. J. and Magill, J. H. *J. Polym. Sci., Polym. Phys. Edn* in press

13 Mujumdar, A. N., Young, S. G., Merker, R. L. and Magill, J. H. *Macromolecules* 1990, **23**, 14
14 Sun, D. C. and Magill, J. H. *Polymer* 1987, **28**, 1243
15 Kojima, M. and Magill, J. H. *Polymer* 1985, **26**, 1971
16 Masuko, T., Okuiziemi, R., Yonetake, K. and Magill, J. H. *Macromolecules* 1989, **22**, 4636
17 Kojima, M. and Magill, J. H. *Polymer* 1985, **26**, 1971
18 Magill, J. H. and Riekel, C. *Makromol. Chem. Rapid Commun.* 1986, **7**, 287
19 Kojima, M. and Magill, J. H. *Polymer* 1989, **30**, 579
20 Magill, J. H. *J. Inorg. Organomet. Polym.* 1992, **2**, 213
21 Singler, R. E., Willingham, R. A., Noel, C., Freidrich, C., Bosio, L. and Atkins, E. D. T. *Macromolecules* 1991, **24**, 510
22 Kojima, M. and Magill, J. H. *Makromol. Chem.* 1992, **193**, 379
23 Young, S. C. and Magill, J. H. *Macromolecules* 1989, **22**, 2549; and to be published
24 Marcelin, G. personal communication, 1989
25 Kojima, M. and Magill, J. H. in preparation